

interpolated data are distributed to the members of the project.

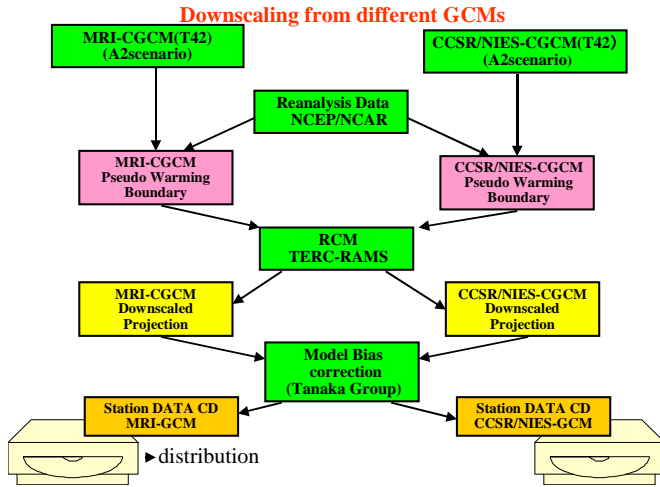


Fig. 2. Flowchart of the downscaling.

3. Simulation of the past climate (hindcast)

Top panel of Figure 3 is nine-year mean monthly observed precipitation in January, during 1994 to 2002. Since precipitation strongly depends on orography, horizontal interpolation is difficult. The bottom of the figure is ten-year mean monthly reproduced (hindcasted) precipitation in January during 1994 to 2003, which is almost corresponding observation shown by the top panel. Horizontal distribution of the hindcasted precipitation agree well to the observation, particularly heavy precipitation along the Black Sea and some areas along the Mediterranean, although precipitation is slightly overestimated. Figure 4 is same as Fig.3 but in April. Observed precipitation distribute quite uniformly although a few stations observing heavy precipitation are scattering along the coastal regions and mountainous areas. The hindcast somewhat overestimate precipitation and shows stronger tendency of stronger precipitation in the coastal and mountainous areas. In July (Fig.5), precipitation becomes minimum in the seasonal cycle. The hindcast agrees well to the observation except for underestimation along the coast line of the Black Sea. The simulated distribution of precipitation also agrees to the observation in October (Fig.6).

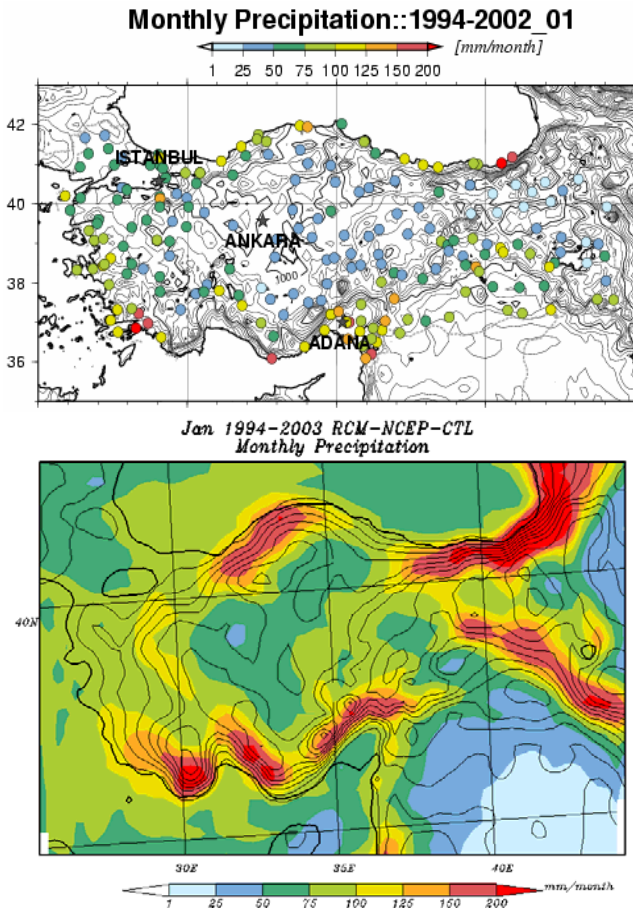


Fig. 3. Ten year mean monthly observed (Top) and hindcast (Bottom) precipitation in January, during 1994-2003, but nine years during 1994-2002 for observation.

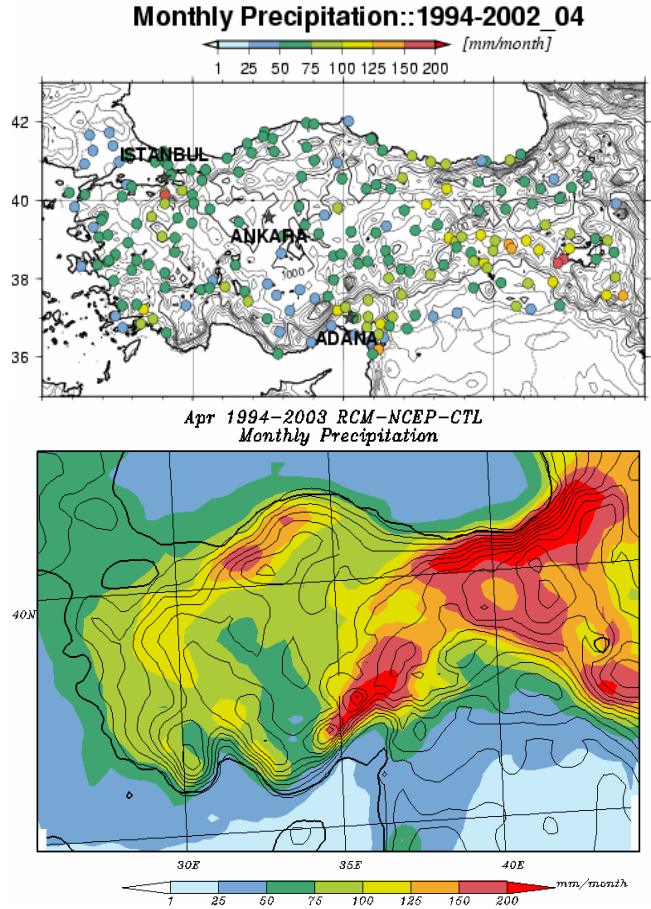


Fig. 4. Same as Fig.3 but in April

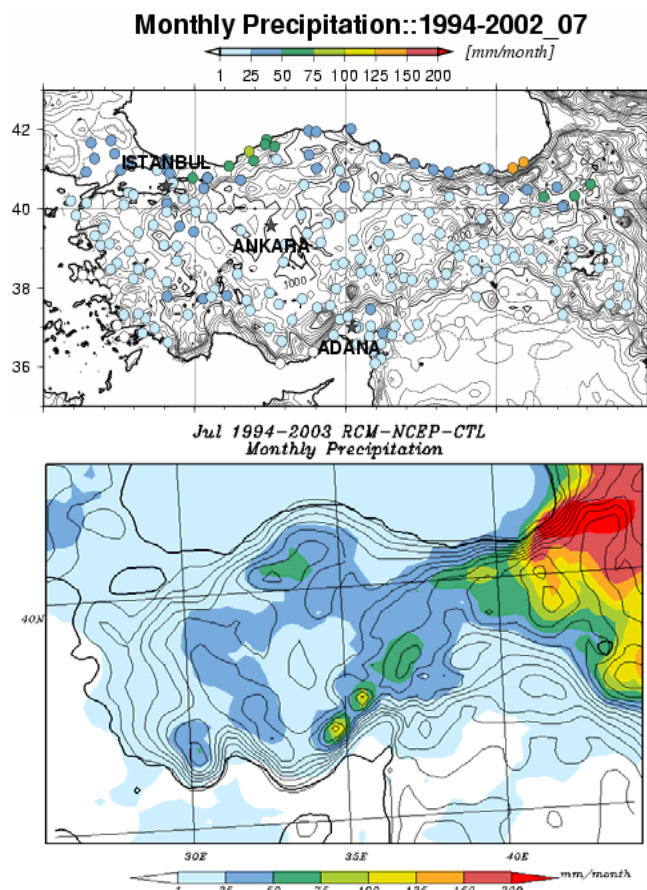


Fig. 5. Same as Fig.3 but in July

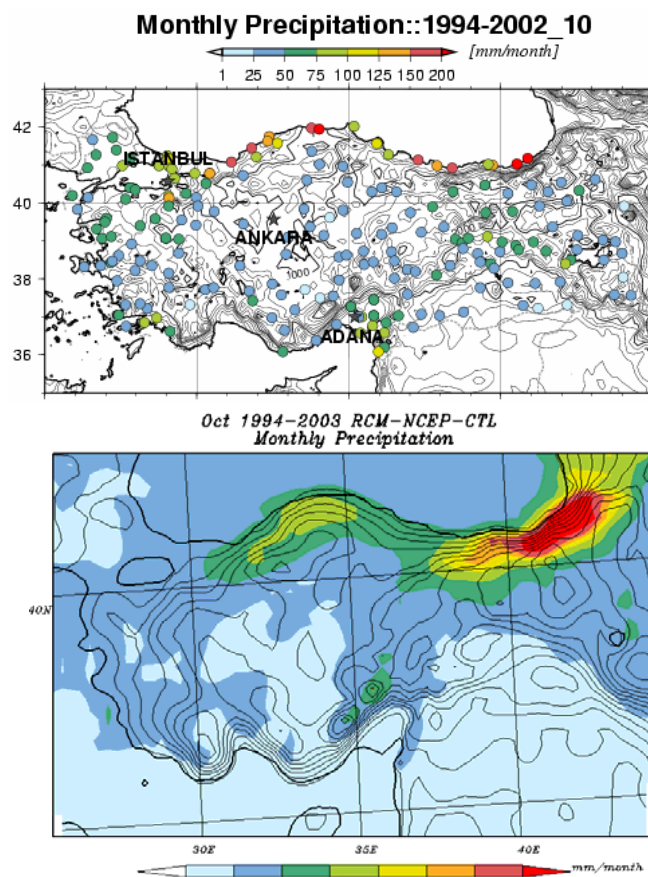


Fig. 6. Same as Fig.3 but in October

Figure 7 shows seasonal cycles of observed and hindcasted precipitation. Observed precipitation is smaller than 20 mm in July, but it exceeds 100 mm in December and keeps about 70 mm during January to April. This is a quite typical seasonal cycle of the Mediterranean climate. The hindcast almost agree well to the observation during May to December. From February to April, in particularly in February and March, hindcast overestimated the amount of precipitation.

Error bars indicate the standard deviation of inter-annual variation of precipitation. The amplitude of inter-annual variation is quite large, especially in November and December. The standard deviations of the control run, namely; hindcast, agree well to the observed ones, but it is overestimated in February to April, when amount of precipitation is overestimated. When the amplitude of inter-annual variation is larger, the estimation of difference in precipitation between the present climate and the future climate becomes difficult because of smaller Signal (climate change) to Noise (inter-annual variation) ratio, i.e., S/N ratio.

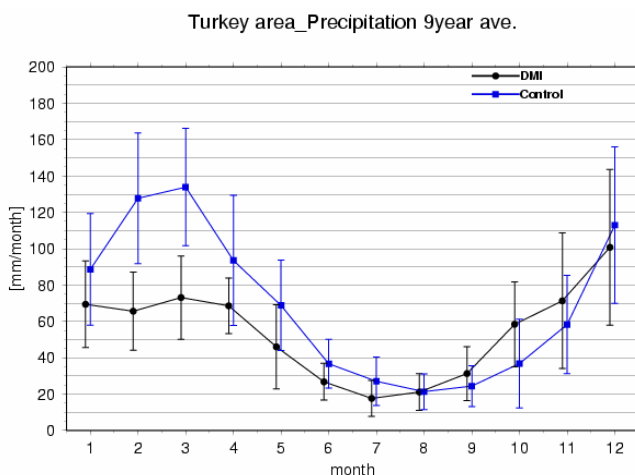


Fig. 7. Seasonal cycles of observed (black, provided by DMI) and hindcasted (blue, by the control run) precipitation. Observed one is the average of 206 in situ stations in the entire Turkey, while the hindcast is average of 206 grid points nearest to the stations in the second grid system. Error bars indicate the standard deviation of inter-annual variation.

4. Projected Precipitation

Figure 8 shows seasonal cycle of the mean monthly precipitation with the downscaled projections by MRI-GCM (red) and by CCSR/NIES (orange). The downscaled precipitation is almost always smaller than that of the control run except for February estimated by downscaling from MRI-GCM. The model predicts that precipitation of Turkey will decrease almost through year. Ratio of the decreasing is prominent during cold season, while decreasing rate is small during summer. Total decreasing rates through year are not so different between those downscaled from MRI and CCSR/NIES, the former is about 27% and the latter is 25%. Note that these differences by the climate change is not always larger than the inter-annual variations, which also are indicated in Fig.9.

Figure 10 shows seasonal cycles of observed and

hindcasted precipitation as well as downscaled precipitation from MRI-CGCM and those from CCSR/NIES-CGCM. Disagreement between observation and estimation by the control run is slightly larger than that of the entire Turkey. The tendency of precipitation change is almost same as that of the entire Turkey, while decreasing in winter is more prominent, especially the downscaling from CCSR/NIES.

Since horizontal distribution of precipitation change in the entire Turkey will be discussed latter, only change around Seyhan basin are discussed here. Figure 11 shows horizontal distribution of difference in precipitation between present and future climate in the finest grid in April. Horizontal pattern of precipitation change between in 1990s and 2070s projected from MRI-CGCM are quite similar to that from CCSR/NIES-CGCM.

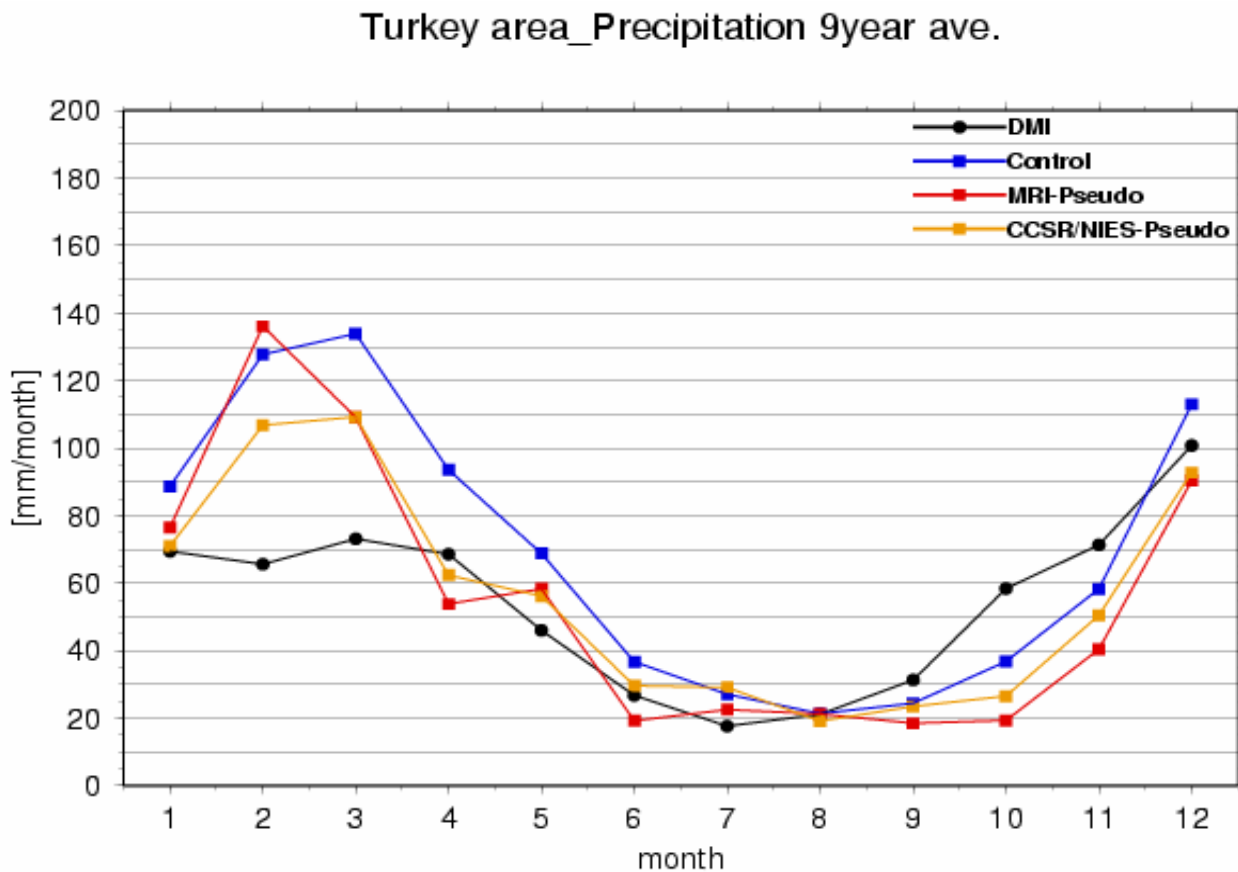


Fig. 8. Same as Fig.7, but for with the downscaled predictions by MRI-CGCM (red) and by CCSR/NIES-CGCM (orange).

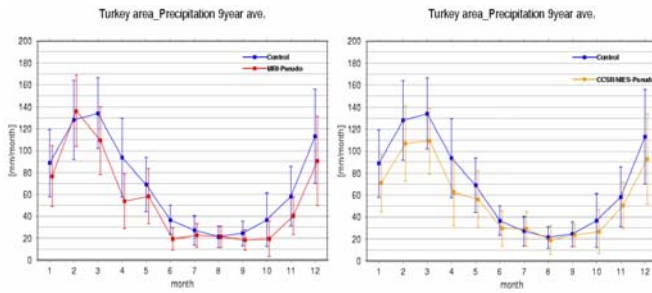


Fig. 9. Standard deviations of precipitation each month (error bars) in the control run (blue) versus downscaling from MRI-CGCM (red, in left panel) and that from CCSR/NIES-CGCM (orange, in the right panel)

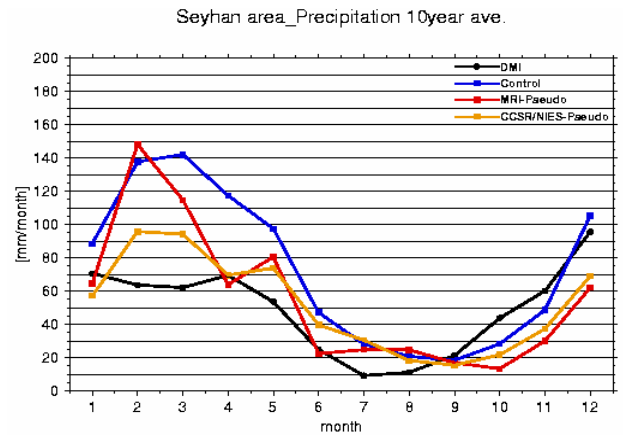


Fig. 10. Same as Fig.8, but mean precipitation in the finest grid (8.3km grid interval)

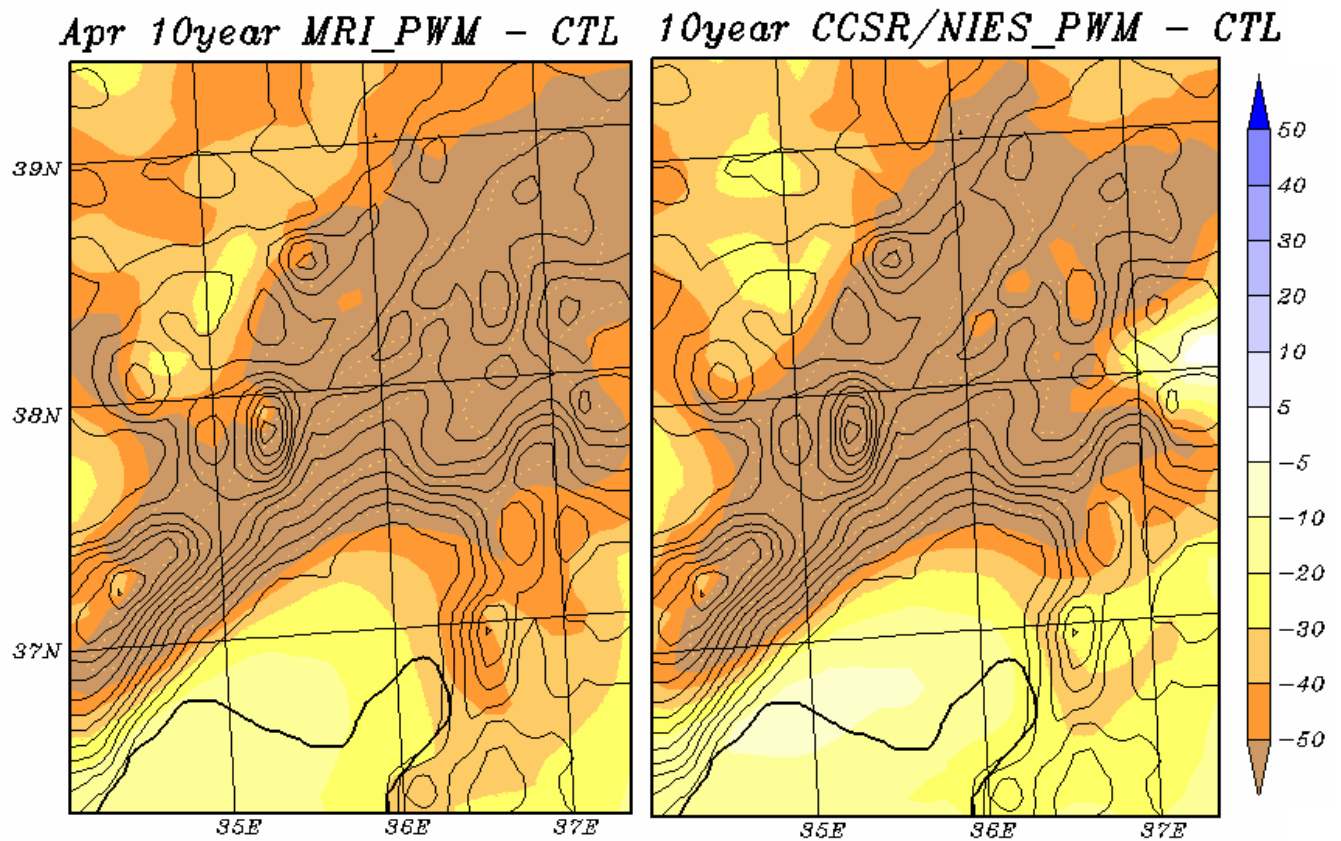


Fig. 11. Horizontal distribution of difference in precipitation between present and future climate in the finest grid downscaled from MRI-CGCM (left) and CCSR/NIES-CGCM (right)

5. Projected extreme events of rainfall

Disasters caused by weather may increase by the effects of climate change. Flood and drought are often the most concerns not only for the farmers but others. Extreme events of daily precipitation and period of no precipitation are good indexes for the potential of these disasters. Figure 12 shows probability density function (PDF) of daily amount of precipitation in four in situ stations. These are statistics of ten years data given by observation (black), control run (blue), downscaling of projection (2070s) by MRI-CGCM (red) and by CCSR/NIES-CGCM (orange). Although accuracy of the control run for the PDF, particularly for the extreme events, depends on the stations, probability up to 32 mm/day are reproduced well. The downscaling from both GCM project that the probability of extreme precipitation will not much change. PDF of the period of no precipitation is shown in Figure 13, in which the vertical axis is number of days of no precipitation periods while horizontal axis indicate the rank of no precipitation period.

No precipitation periods given by the control run and observation at Adana has large discrepancy in the long duration. Others are mostly agree well. The change in PDF of long no-precipitation periods are not so different between present climate and future climate. We are not sure that these results are reliable or not. The meaning of the extreme events estimated by PGWM should be studied in the future.

6. Projected Temperature

Figure 14 shows seasonal cycles of observed and hindcasted surface level air temperature. Temperature estimated in the control run has cold bias, particularly in the warm season. Inter-annual variability is larger in the cold season and spring. Projected seasonal cycles are shown in Figure 15. Both downscaling indicate increase of surface temperature in all months. Seasonal variation of the difference is quite small as well as the inter-annual variation which is indicated in Figure 16. The range of differences projected by the downscale from CCSR/NIES- CGCM is much larger than that of MRI-CGCM. The former projects to increase by about 2.0K, while latter by about 3.5K. The large difference between two downscaling is a faithful reflection of the difference of GCMs. The change in temperature is quite similar to the projection in the finest grid as shown in Figure 17.

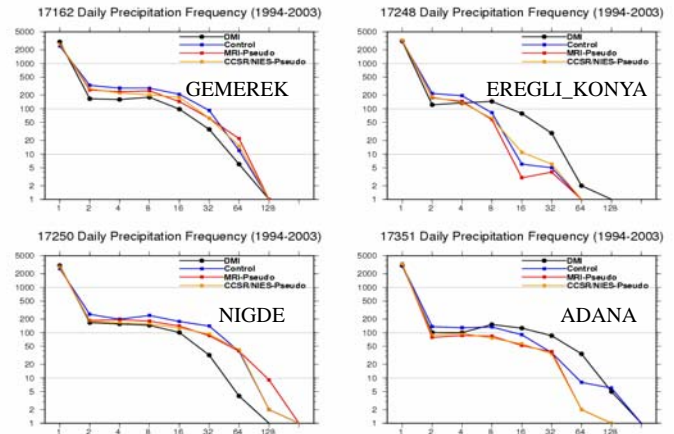


Fig. 12. Probability density function of daily amount of precipitation in four in situ stations. The vertical axis is number of days during 10 years and the horizontal axis is daily precipitation. Black line indicate observed PDF other three colors are the same as Fig.8.

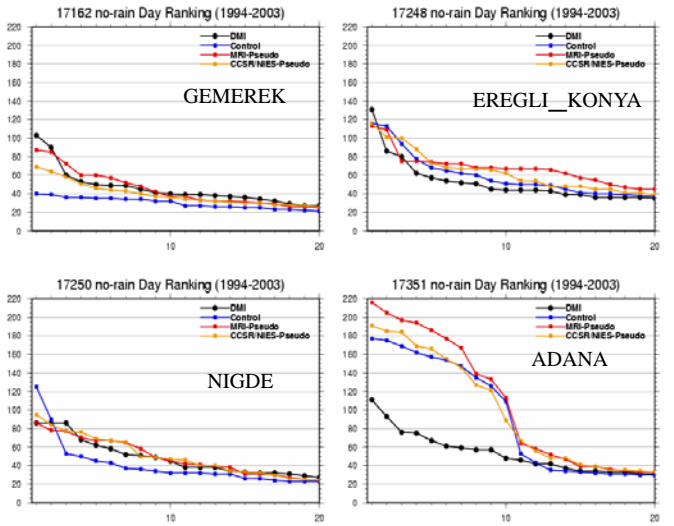


Fig. 13. The longest period of no precipitation. Vertical axis: number of days of the period of no precipitation. Horizontal axis: the rank of the longest period

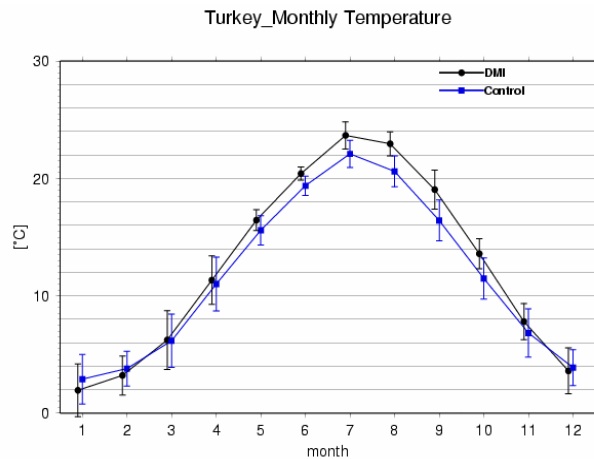


Fig. 14. Same as Fig.7, but for Temperature

Turkey_Monthly Temperature

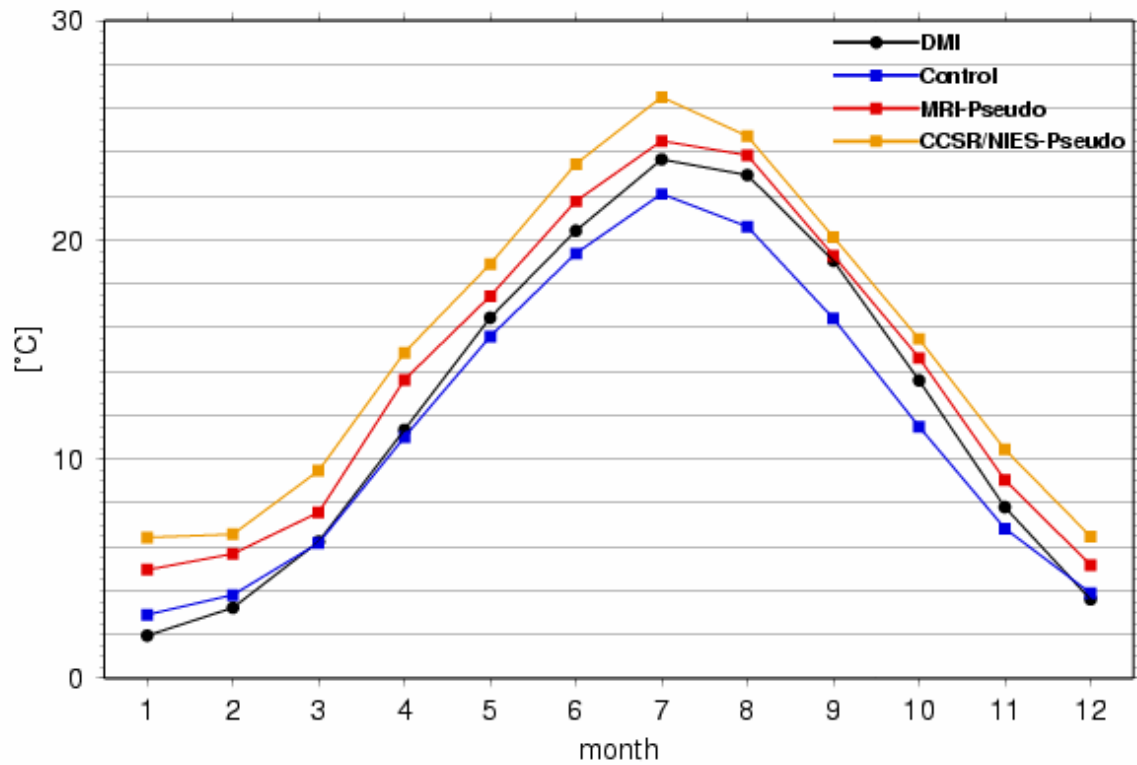


Fig. 15. Same as Fig.8, but for Temperature

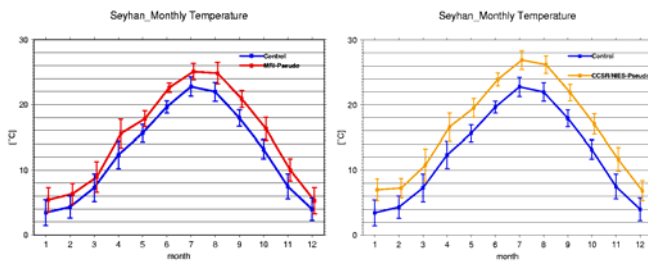


Fig. 16. Same as Fig.9, but standard deviations of temperature

Figure 18 shows horizontal distribution of difference in surface temperature between present and future climate in the second grid and the finest grid of downscaling from MRI-CGCM in the top and bottom panels, respectively. Temperature change is larger in the southern part of Turkey, particularly in the mountainous area along the Mediterranean. The change is large also in the south western part of Turkey. The bottom panel indicates that the change is relatively small along the coast in Adana plain, while it is larger in the surrounding mountains, showing a tendency of stronger warming in the southern slopes. Projection based on CCSR/NIES-CGCM shows much stronger increase of surface temperature. Figure 19 indicates that the difference will exceed 3.0K in the most part of Turkey.

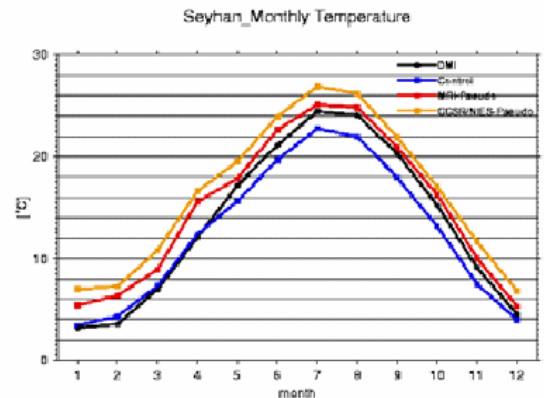


Fig.17: Same as Fig.10, but for mean surface temperature in the finest grid

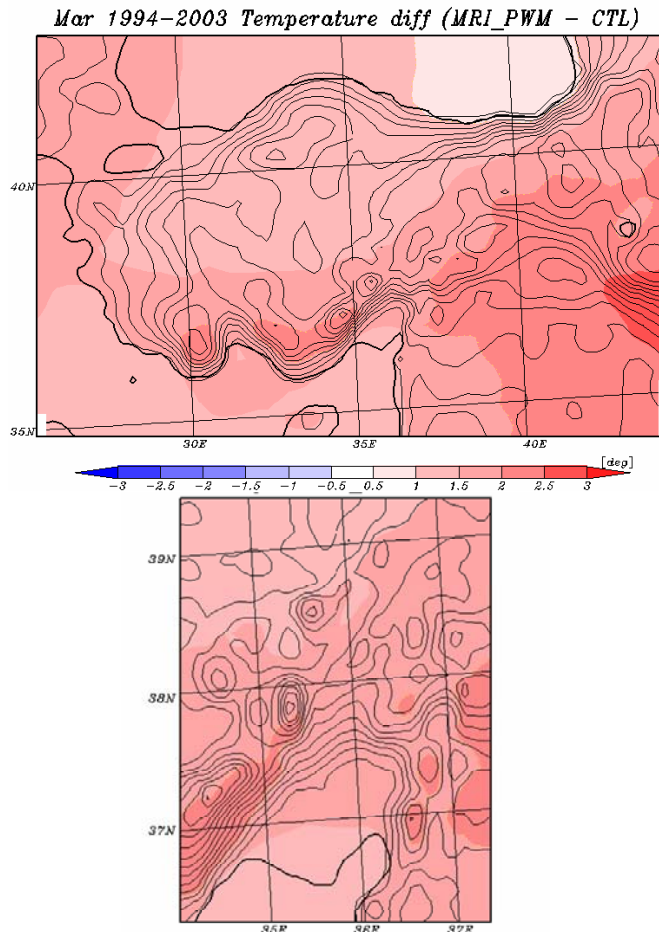


Fig. 18. Horizontal distribution of difference in surface temperature between present and future climate in the second grid (top) and the finest grid of downscaling from MRI-CGCM

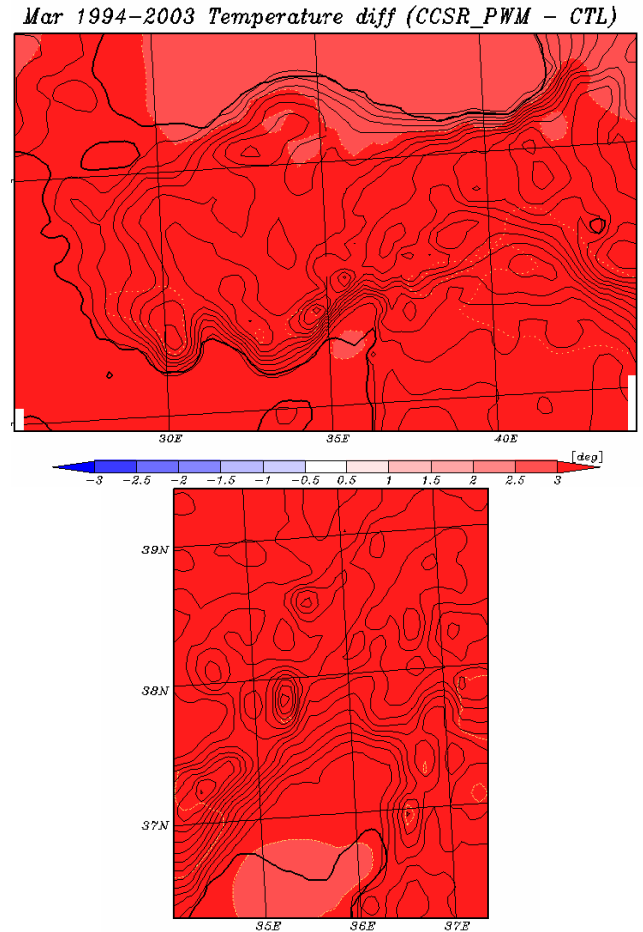


Fig. 19. Same as Fig.18, but for CCSR/NIES-CGCM

7. Projected Insolation

Figure 20 shows monthly mean daily total insolation (MJ/m^2) at Adana during the period of January 1994 to December 1996. Although the control run overestimate in the warm season, it agrees to observation in cold seasons. The change between 1990s and 2070s are very small. Only some difference can be seen in the cold season, in which it frequently becomes cloudy and rainy. Figure 21 shows horizontal distribution of monthly

mean daily total insolation in March. Insolation change is also affected by orography. Insolation change is larger in mountainous area in April but weaker in August. This fact is related to distribution of precipitation.

Monthly daily total solar radiation Adana (a)

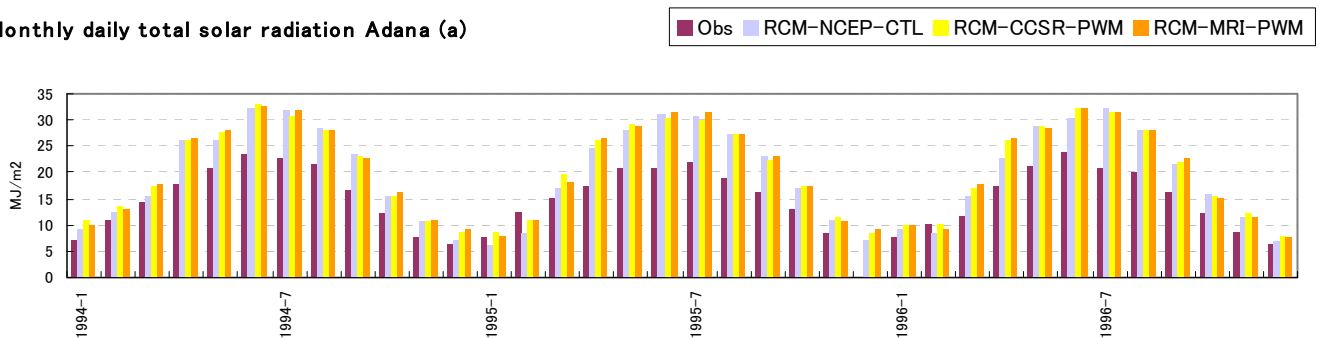


Fig. 20. Monthly mean daily total insolation (MJ/m^2) at Adana. Brown bars: observation, gray: control run, yellow: downscaled from CCSR/NIES, orange: MRI

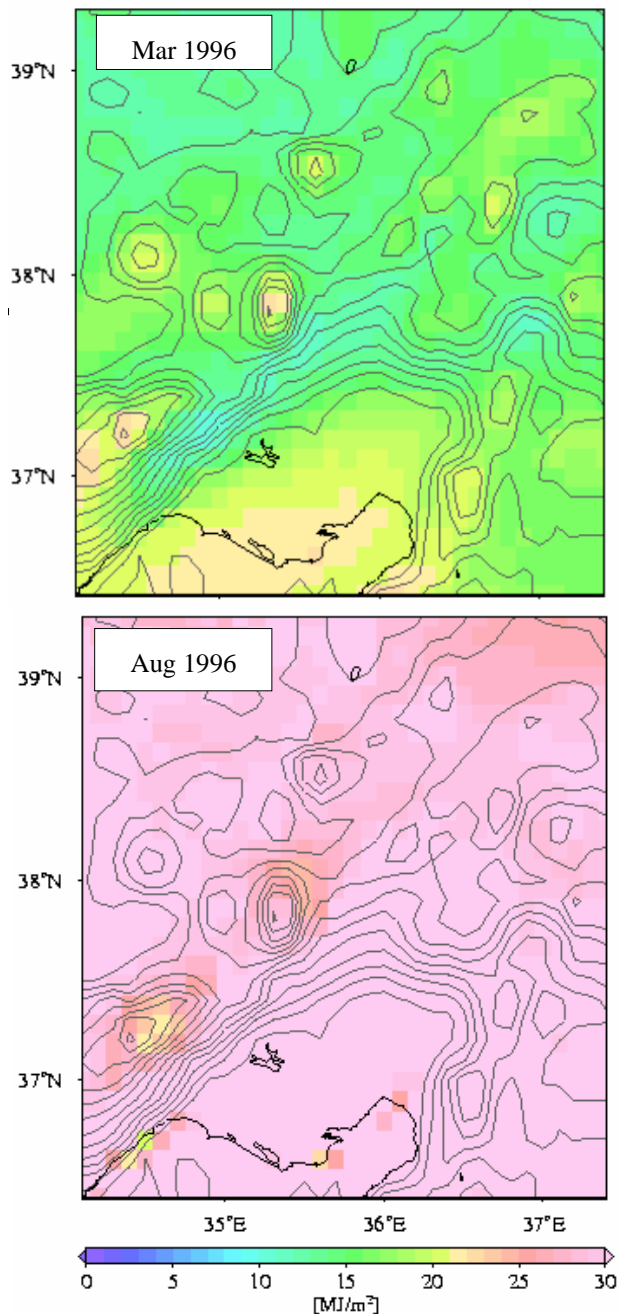


Fig. 21. Horizontal distribution of monthly mean daily total insolation in March (top) and August(bottom) in 1996.

8. Comparison to the projections by GCMs.

To assess the reliability of the downscaling, comparison between different models is useful. Kitoh (2007) presented some climate projection in Turkey by Global Climate Models. Since precipitation reflects generally quite well the characteristic of the model, projected change in precipitation is compared here. Figures 22 to 24 are comparison to some other projections presented by Kitoh (2007) as an individual report of the Climate Group of IPCC. Top left panel of Fig.22 is the projection by AOGCM (resolution is about 200km) and top right panel is that of CGCM (TL959) with 20km horizontal resolution shown in his report. These are precipitation difference during December, January and February between the present period (1981-2000) and future period (2081-2100) assuming the SRES A1B scenario. Although the comparing periods and scenario is different from the downscaling, the results are expected to have high similarity to those under same conditions as the scenario we assumed. AOGCM indicates decreasing of precipitation especially in the southern part of Turkey. CGCM (TL959) shows increasing in precipitation along the coast of the Black Sea but decreasing along the coast of Mediterranean. The two downscaled projection, lower left panel (MRI-CGCM) and lower right panel (CCSR/NIES-CGCM), are quite similar to those of CGCM (TL959). The downscaled projection also have some similarity to the results of AOGCM, although resolution is quite different.

On the other hand, during spring, March, April and May (Fig. 23), we can not see any similarity between two downscaling and CGCM (TL959). Two downscaling are quite similar each other and AOGCM has also some similarity. During summer (Fig. 24) and autumn (Fig. 25), no similarity can be seen between two downscaling and CGCM (TL959). Particularly downscaling from CCSR/NIES-CGCM has an opposite pattern against the projection by CGCM (TL959) in October and November. On the other hand, two downscaling keep some similarity to AOGCM in spring and winter. Similarity between AOGCM and downscaling from MRI-CGCM has been previously expected because this GCM is basically same as the source of the downscale, i.e., MRI-CGCM. On the other hand AOGCM and the downscaling from CCSR/NIES-CGCM are completely independent each other. These two seem to agree well each other.

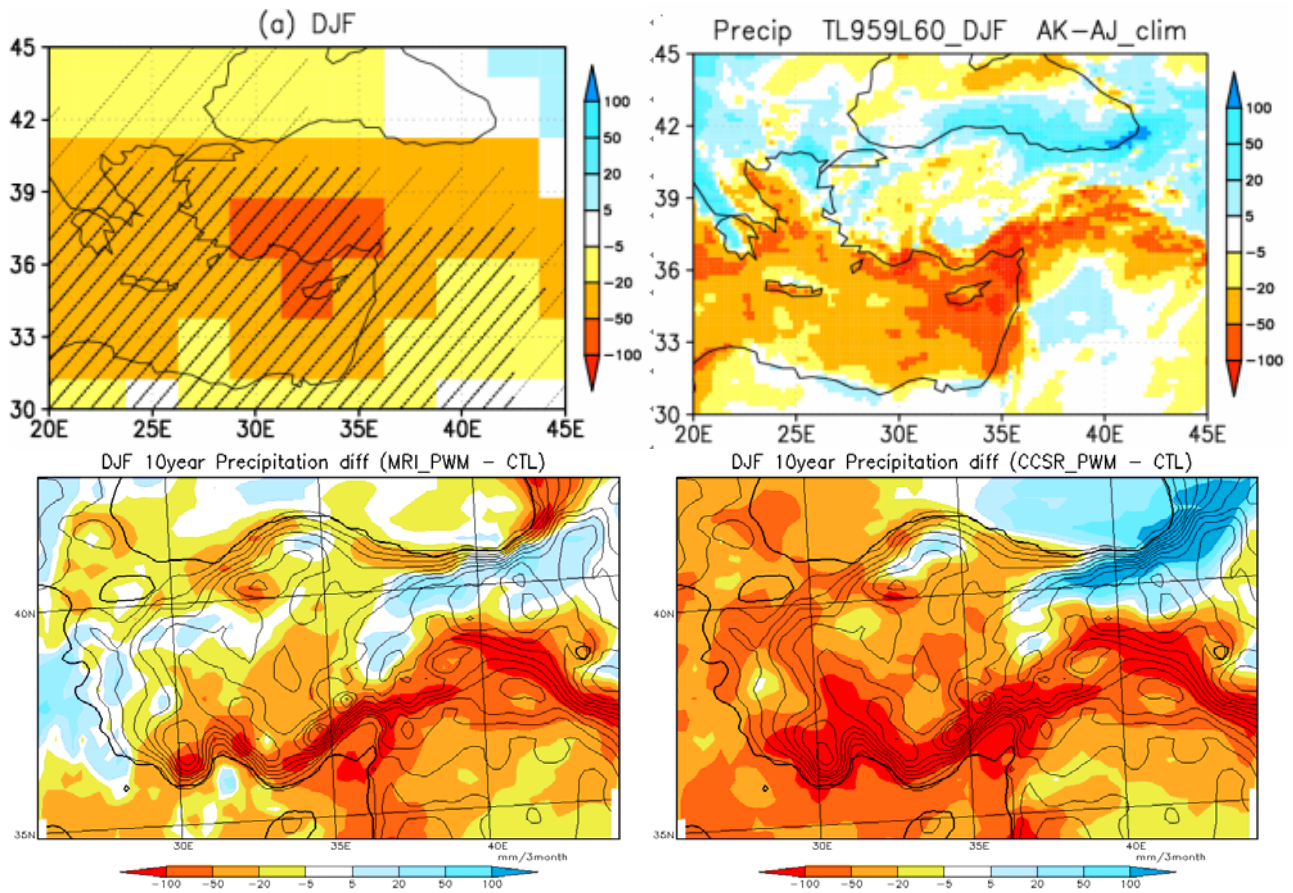


Fig. 22. Projected precipitation change in December, January and February. Top left: AOGCM, top right: CGCM(TL959), the lower left panel: downscaling from MRI-CGCM, lower right panel: downscaling from CCSR/NIES-CGCM.

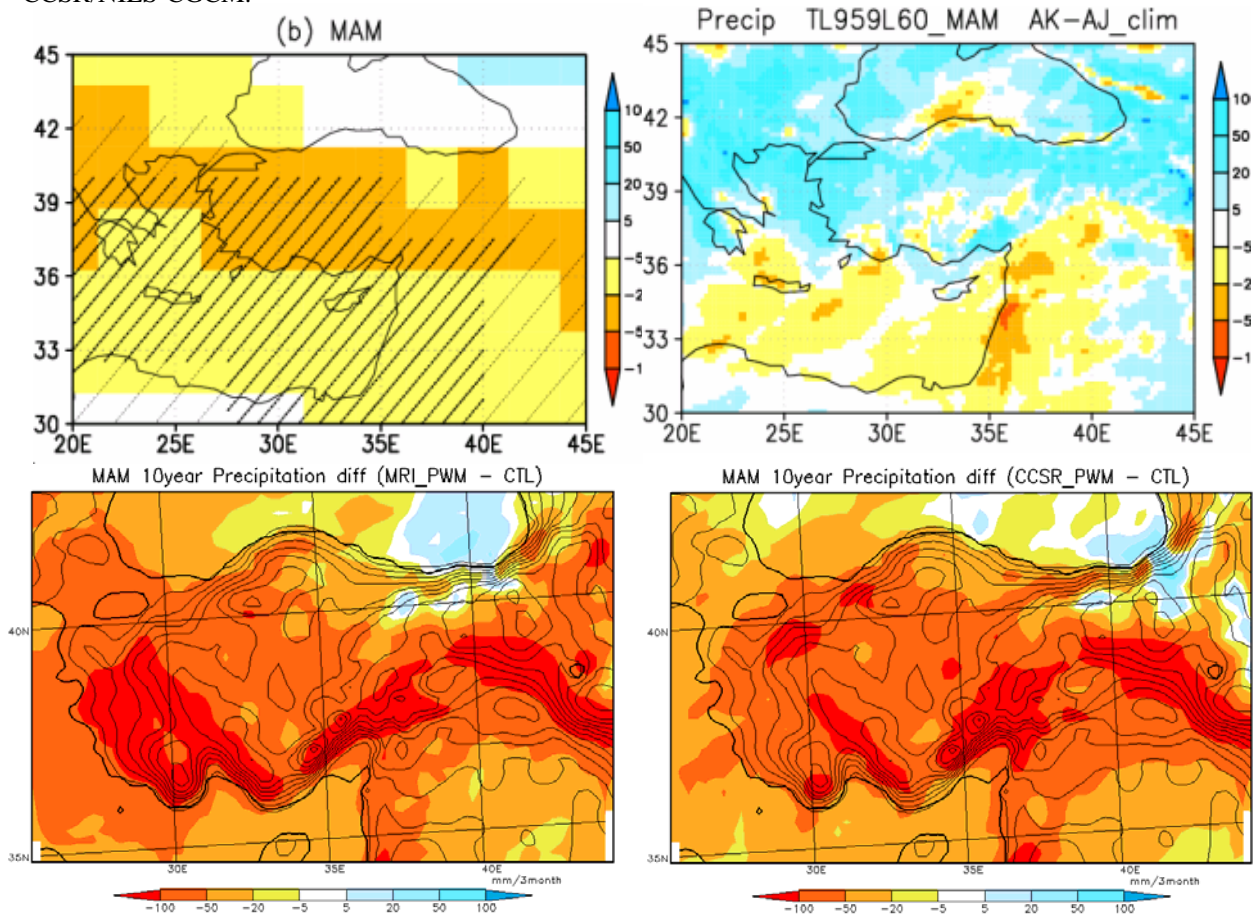


Fig. 23. Same as Fig.22, but for March, April and May

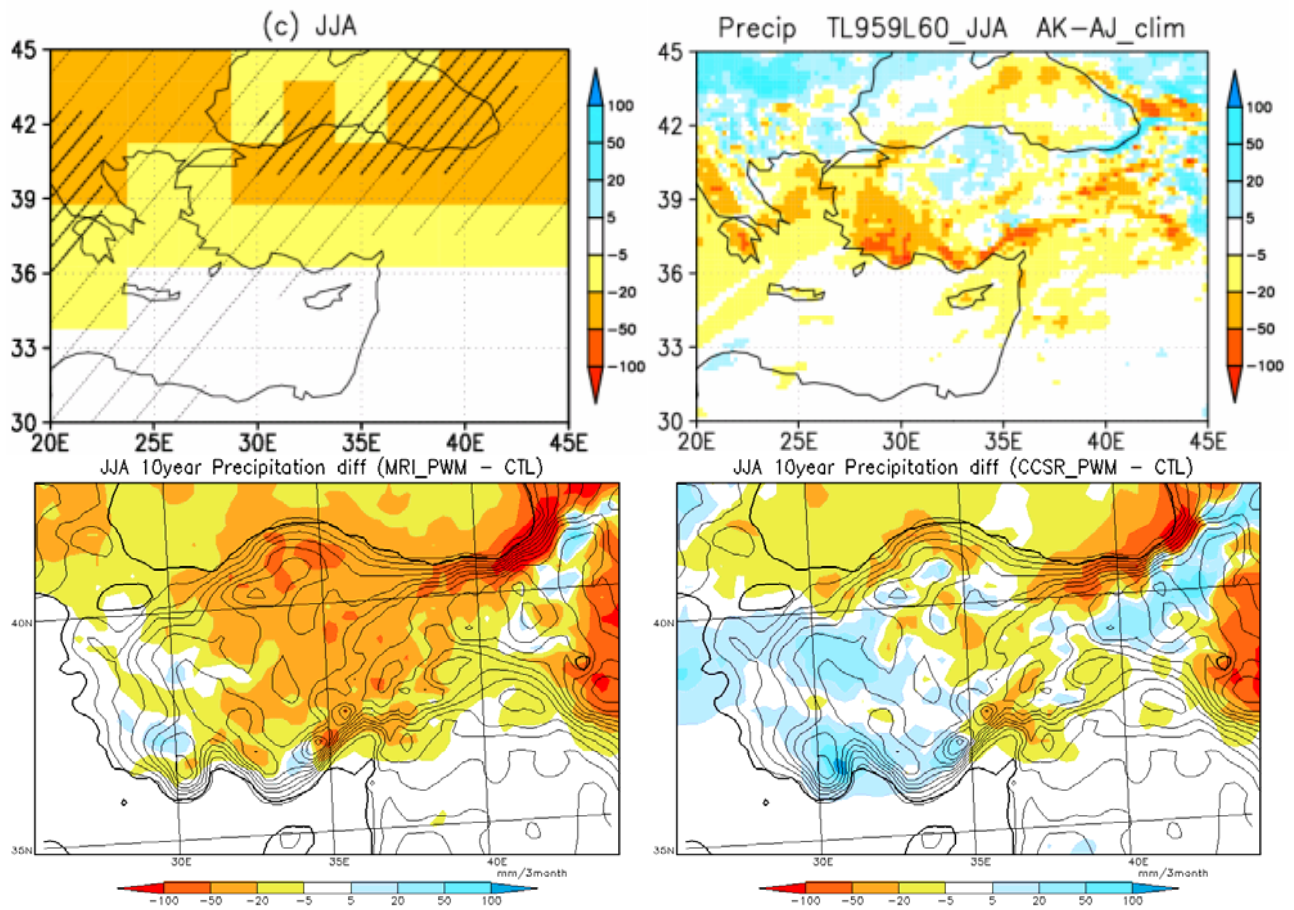


Fig. 24. Same as Fig.22, but for June, July and August

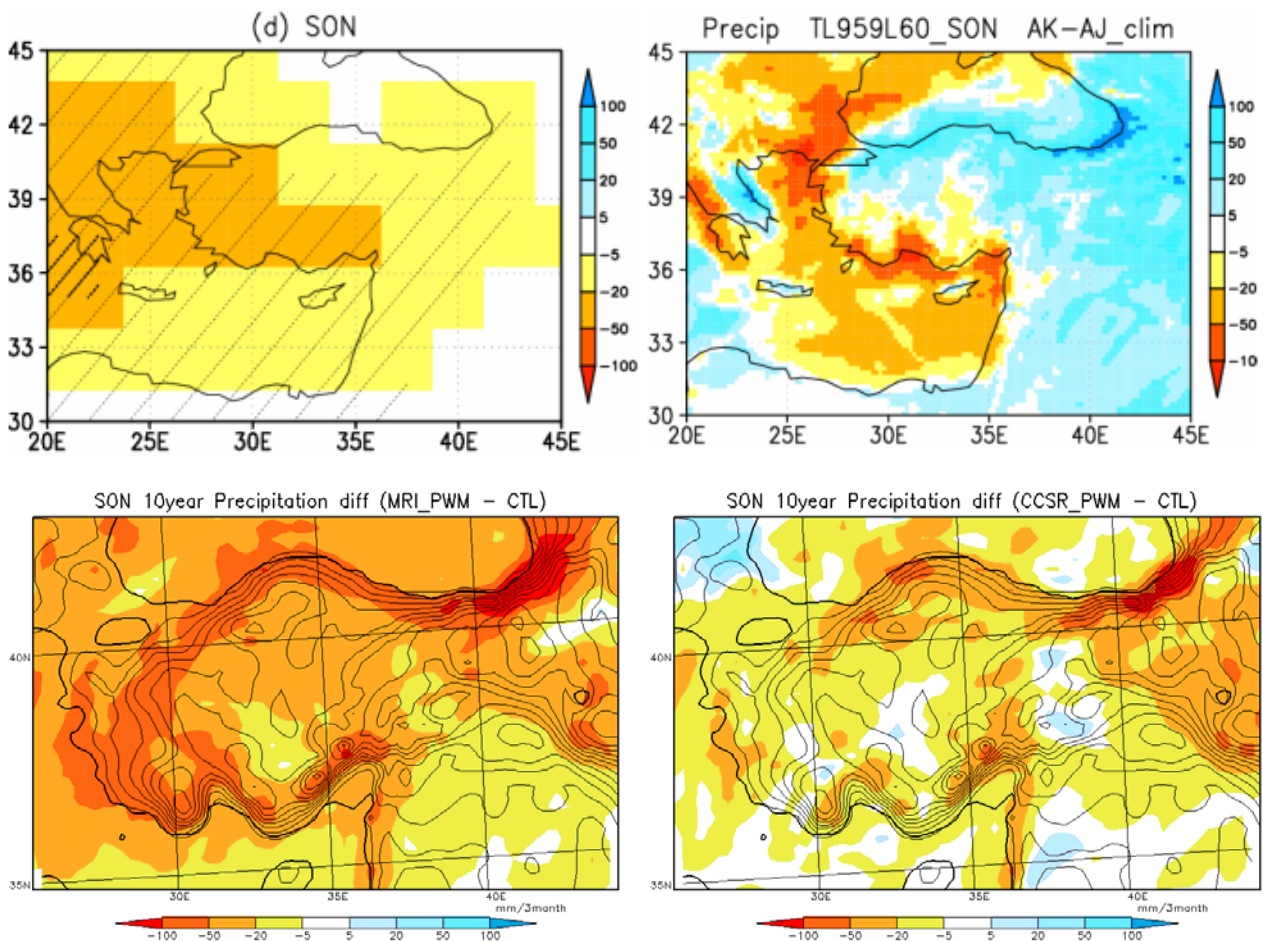


Fig. 25. Same as Fig.22, but for September, October and November

9. Conclusions

Control run of RCM tends to overestimate precipitation during winter. RCM has cold bias in surface temperature because of the numerical scheme for the dynamics over steep slopes, while this effects are limited in the lowest atmosphere and only when wind is strong and the lower atmosphere is strong stable condition.

The downscaling suggests that precipitation will decrease 10-40 mm/month during cold season in 2070s. Precipitation change has good similarity between two downscaling projections using MRI and CCSR/NIES GCMs. Amount of precipitation is strongly affected by the orography, as the result, the change in precipitation is also affected by the orography. Decreasing of precipitation is more prominent in the slopes along the Mediterranean. Temperature change strongly depends on GCMs. Surface temperature increase by 2.0K (MRI-GCM) to 3.5K (CCSR/NIES-GCM). Temperature change is also clearly affected by the topography. The change is larger in the southern part of Turkey, particularly in the mountainous area along the Mediterranean. Independent two projections of precipitation, using MRI-AOGCM and CCSR/NIES have some similarity in horizontal distribution, but they are quite different from the projection by the high-resolution CGCM (TL959), which must be currently one of the most advanced projection method in the world for the regional climate change. We have to say that the reliability of the small scale projection is still not very high.

10. References

- Wang, Y., L. R. Leung, J. L. McGregor, D. -K. Lee, W.-C. Wang, Y. Ding, and F. Kimura, 2004: Regional climate modeling: Progress, Challenges, and Prospects. *J. Meteor. Soc. Japan.*, 82, 1599-1628.
- Kimura, F. and A. Kitoh, 2007: Downscaling by Pseudo Global Warning Method, Final report of ICCAP.
- Kitoh, A. 2007: Future Climate Projections around Turkey by Global Climate Models, Final report of ICCAP.
- Yukimoto, S., A. Noda, A. Kitoh, M. Sugi, Y. Kitamura, M. Hosaka, K. Shibata, S. Maeda and T. Uchiyama, 2001: A new Meteorological Research Institute coupled GCM (MRI-CGCM2) - its climate and variability -. *Pap. Met. Geophys.*, 51, 47-88.
- K-1 Model Developers, 2004: K-1 coupled model (MIROC) description. K-1 Technical Report 1 [Hasumi, H. and S. Emori (eds.)], Center for Climate System Research, University of Tokyo, Tokyo, Japan, 34pp.
- <http://www.ccsr.u-tokyo.ac.jp/kyosei/hasumi/MIROC/tech-repo.pdf>